Cell Model Theory of Homogeneous Fluidization: Density and Viscosity Behavior

JAMES A. SAXTON, JOHN B. FITTON, and THEODORE VERMEULEN

University of California, Berkeley, California

As a step toward a unified treatment of particulately fluidized beds, a statistical-thermodynamic approach has been investigated, with the smoothed potential cell theory of pure liquids used to establish an equation of state and a collisional-viscosity relation. This treatment has correlated well with experimental data on liquid-fluidized beds, and the same method gives reasonable predictions for gas-fluidized beds. A parameter equivalent to thermodynamic temperature has been identified for fluidized beds, which depends solely upon fluid properties and includes the three-halves power of superficial velocity. This approach should be of value for interpreting other liquidlike properties of fluidized systems.

The premise of this investigation is that the similarity between monatomic liquids and particulately fluidized beds of uniform spherical particles is sufficient to justify the employment of each as a model or analogue for the other.

In steady state fluidization, on the average, the downward force of gravity on the particle is matched by the upward drag force of the fluidizing medium (the ether). The gravitational force corresponds to an attractive force between particles, while the fluid drag presents a direct analogy to repulsive forces on the molecular level.

This analogy extends to the bulk behavior of the bed, from the fixed-bed state at low velocity to the terminal velocity where the particles are transported from the system. These two limits bear a striking resemblance to the phenomena of fusion or glass transition (*12*) and of evaporation. Between these two limits, continuous expansion occurs, showing direct similarity to the thermal expansion of liquids. Throughout this expansion the bed has a relatively quiescent free upper surface, with few if any particles attaining sufficient energy to rise above it; in this sense the bed resembles a liquid having a low vapor pressure. In addition, the surface when disturbed will support wave propagation, so that a finite surface tension may be associated with it. Phase separation and partial miscibility for particles of different sizes or densities have also been observed, in behavior similar to that given by regular solution interactions in liquids.

The glass-transition analogy has been proposed because the settled fluidized bed is random in structure, rather than ordered. However, the properties treated here are those of the molten state, not of the solid. A molten glass is polymeric and seems to resemble a fluidized bed much less than does a monatomic liquid.

The viscous behavior of fluidized beds has been widely studied (*1, 5, 9, 10, 16, 19, 22, 27, 29*). For uniform fluidization it has been found that the apparent viscosity of the beds decreases with increased velocity of the fluid medium. Thus, if the vibrational (thermal) energy of the fluidized bed is directly related to the kinetic energy of the fluidizing medium, then the thermal behavior of the fluidized-bed viscosity resembles that of liquids rather than gases.

All current liquid theories consider that molecular interaction takes place only among particles in a subsystem; that is, a given molecule interacts with n ($n << N$) particles in an average potential field established by the ($N - n$) other particles. The justification for this assumption lies in the experimental observation that while liquids possess short-range order among molecules in the subsystem, there is negligible long-range order.

These theories fall into two general categories. One employs knowledge of the radial distribution of molecules around a central molecule, which is established by experimental or theoretical means, to predict the thermodynamic properties; the other postulates that a hypothetical cage exists around each molecule, with suitable choice of properties for the environment within the cell leading to quantitative predictions of liquid behavior. The latter model appears to be more usable for purposes of the present study.

THERMODYNAMIC ANALYSIS

Free Volume (Cell Model) Theory

The motion of a molecule in a liquid can be described as a random walk between successive groups of contiguous molecules. Between intergroup jumps, the molecule oscillates within the potential barrier or three-dimensional cell formed by the neighboring molecules. Normally the frequency of oscillation within each cell is much greater than the frequency of the intercell jumps, and hence the thermodynamic properties of the liquid will be largely determined by the cell properties. The problem, then, is to determine the effective potential-energy field within a cell in order to establish the cell partition function and thermodynamic properties related to it.

The free volume approach, first suggested by Eyring and Hirschfelder (*7, 8*), describes a liquid as being composed of individual molecules, each moving in an average potential field created by its neighbors. The resulting partition function for each molecule can be written as

$$z = Z^{1/N} = z_{\text{int}} \frac{v_f \exp\left[-\omega/(kT)\right]}{\Lambda^3} \tag{1}$$

This equation serves to define the free volume as the effective liquid-phase volume within which a molecule will obey the perfect gas law, $pv_f = kT$. The resulting state properties may be obtained readily from statistical thermodynamics (*21*):

$$E = \frac{3}{2}NkT + N\omega + NkT^2\left(\frac{\partial \ln v_f}{\partial T}\right)_v \tag{2}$$

$$S = Nk \ln (v_f/\Lambda^3) + \frac{3}{2}Nk + NkT\left(\frac{\partial \ln v_f}{\partial T}\right)_v \tag{3}$$

$$F = N\omega - NkT \ln (v_f/\Lambda^3) \tag{4}$$

$$p = -N\left(\frac{\partial \omega}{\partial V}\right)_T + NkT\left(\frac{\partial \ln v_f}{\partial V}\right)_T \tag{5}$$

Eyring empirically related the microscopic variables ω

James A. Saxton is with Bellcomm, Inc., Washington, D. C. John B. Fitton is with Chevron Research Co., Richmond, California.

and v_f to the volumetric properties of the liquid. In an alternative approach, Lennard-Jones and Devonshire (*17*) related ω and v_f to the intermolecular force constants of the molecules. They postulated that since the field acting upon a molecule rapidly fluctuates, it could be represented by an average field possessing spherical symmetry. In that case, the mean energy of a molecule's interaction with its neighbors depends only upon its radial distance from the center of the cell; $\omega = \omega(r)$. If the energy of the system with all particles at the centers of their cells is chosen as the reference state, the partition function is

$$Z = \frac{v_f^N}{\Lambda^{3N}} \exp\left[-\frac{N\omega(0)}{2kT} \right] \quad (6)$$

where

$$v_f = 4\pi \int_{\text{cell}} \exp\left[-\{\omega(r) - \omega(0)\}2kT \right] r^2\, dr \quad (7)$$

In this treatment, the free volume v_f serves as the cell partition function; $N\omega(0)/2$ is the system energy when all particles are at the centers of their cells.

By assuming a form for the intermolecular potential, for example, the Lennard-Jones 6-12 potential, the mean energy can be evaluated as a function of radius in a straightforward manner. The resulting expression can be represented functionally by

$$\omega(r) = A\ \epsilon^*\ \Phi\left[(d/a), (r/a)\right] \quad (8)$$

The thermodynamic functions are again as given in Equations (2) to (5), where ω is now defined equal to $\omega(0)/2$.

Modifications of this cell model give rise to two widely used cases, the hard sphere and square well models. The hard sphere model postulates billiardlike molecules which interact with an infinite repulsive force upon contact, but experience no potential field between collisions. The molecular energy within the cell is, thus

$$\omega(r) = 0 \qquad 0 \leq r < (a - d) \quad (9)$$

$$\omega(r) = \infty \qquad r \geq (a - d) \quad (10)$$

A square well model developed by Prigogine, designated as the *smoothed potential* approximation, offers further improvement, yet possesses the simplicity of form necessary for analytic calculations. It assumes that the molecule in its cell is acted upon by a uniform potential given by the molecular potential of the molecule when located at the cell center. Physically, such an assumption is justified by the fact that while a molecule's interaction with some molecules increases when it moves away from the cell center, its interaction with other molecules decreases, and in the range of liquid densities these two effects tend to compensate. The model continues to exhibit infinite repulsive force during molecular contact, and the reference potential energy $\omega(0)$ is generally calculated by averaging a Lennard-Jones 6-12 potential. The form of the cell potential with respect to the reference potential is identical to that for hard spheres; that is

$$\omega(r) - \omega(0) = 0 \qquad 0 \leq r < (a - d) \quad (11)$$

$$\omega(r) - \omega(0) = \infty \qquad r \geq (a - d) \quad (12)$$

Thus, the same partition function results for both cases, with v_f given by

$$v_f = \frac{4}{3}\pi\,(a - d)^3 = \frac{4}{3}\pi\gamma\,(v^{1/3} - v_0^{1/3})^3 \quad (13)$$

where γ is defined by $\gamma = a^3/v = d^3/v_0$ (for example, $\gamma = \sqrt{2}$ for a face centered cubic lattice). The agreement of this equation of state with numerical calculations by the Monte Carlo method is quite good (*24*).

The equation of state for the hard sphere model is

$$p = kT/[v^{2/3}\,(v^{1/3} - v_0^{1/3})] \quad (14)$$

This relation does not contain the volumetric dependence of the reference potential that is exhibited by the square well model:

$$p = -\frac{1}{2}\,[\partial\omega(0)/\partial v]_T + kT/[v^{2/3}\,(v^{1/3} - v_0^{1/3})] \quad (15)$$

The last term in Equation (15), the kinetic pressure, arises from the molecular motion of the hard spheres, and the middle term, the internal pressure, results from the configurational (that is, position dependent) interaction between molecules.

Collisional Viscosity

Collisional expressions for the transport of momentum and energy in a dense gas have been developed by Collins and Raffel (*4*). These authors established an expression for the pressure tensor of a hard sphere fluid from statistical-mechanical considerations. Relationships for the collisional pressure and the shear and bulk viscosities were then abstracted from a comparison of the terms in this pressure tensor with equivalent terms in the general phenomenological pressure tensor for a Newtonian fluid. This comparison of terms led to

$$\eta = \frac{2}{5}\, d_p \left(\frac{mkT}{\pi}\right)^{1/2} \left(\frac{p}{kT} - \frac{1}{v}\right) \quad (16)$$

The internal pressure does not contribute, since there is no action at a distance in a hard sphere or smoothed potential fluid.

Statistical Temperature in Fluidized Bed

The Collins-Raffel model for viscosity as given by Equation (16) and the kinetic pressure given by Equation (14) or (15) can be combined to provide an explicit relation for the statistical temperature of a hard sphere fluid:

$$kT \equiv \Theta = \frac{37.5}{\Delta\rho\ d_p^5} \left[\frac{v^{1/3} - v_0^{1/3}}{v_0^{1/3}}\right]^2 (\eta v)^2 \quad (17)$$

In deriving Equation (17) for a fluidized bed, the effective particle mass is taken as $\pi\, d_p^3\, \Delta\rho/6$. (The question arises whether the gross particle density ρ_s or the net particle density $\Delta\rho$ is the proper term to use here; dimensional analysis appears to support $\Delta\rho$.)

It is desirable to consider what properties a fluidization variable must possess to be equivalent to thermodynamic temperature. One way to describe this function is a statistical quantity that must be essentially the same, at any given instant, for any two vicinal elements or samples of a system in equilibrium.

According to the concept of thermal equilibrium, if two particle systems are intermingled or adjacent, their temperatures should become the same. For such thermal equilibrium to occur in the case of dissimilar particle types (for example, those differing in size, shape, or density), the fluidization parameter equivalent to thermodynamic temperature must depend solely upon fluid properties. In particular, the temperature should be the same for particles so dissimilar that they form separate immiscible layers which are in contact across a horizontal interface. Therefore, the criterion of no dependence on particle properties will be set as an essential requirement in our development of a nominal temperature function for the fluidized bed.

It seems logical to identify the flow energy of the fluid as the source of heat or energy in the fluidized bed. A measure of the nominal temperature may be gained, then,

in two equivalent ways. First, it is the temperature, in energy units, associated with the particles; alternatively, it is the effective thermal energy of the medium with which the particles are in equilibrium. Viewed from the latter standpoint, the nominal temperature Θ may well be related to the kinetic energy of the fluid in the bed, ρU^2. The requirement that Θ depend solely upon fluid properties may be functionally stated as

$$\Theta = \Theta(\rho,\ \mu,\ g,\ U_0)$$

Dimensional considerations for the general case, where Θ is proportional to an unknown power of the superficial velocity, suggest that Θ is given by the product

$$\Theta = \psi \left(\frac{\mu^2\ U_0^2}{\rho g} \right) \left(\frac{\mu g}{U_0^3\ \rho} \right)^m \qquad (18)$$

It is of interest to compare Equation (18) with the nominal temperature expressions of three other investigators who have related fluidized beds to liquids. Furukawa and Ohmae (*10*), basing their arguments upon a harmonic-oscillator model and empirical considerations, postulated that the nominal temperature should be proportional to μU_0. While this function exhibits the necessary independence from particle properties, several steps in its development were somewhat arbitrary; also, it was not applied in a consistent manner to interpret those authors' fluidized-bed experimental data on expansion, viscosity, surface tension, and miscibility behavior.

Schügerl et al. (*27*), by comparing their correlation of gas-fluidized-bed viscosities with Eyring's rate-theory expression, arrived at the relation

$$\Theta = \frac{a}{2n\ \delta_0} \frac{U_{mf}(U_0 - U_{mf})}{C_4\ d_p^4} \qquad (19)$$

The minimum fluidization superficial velocity U_{mf} is

$$U_{mf} = \frac{(\Delta\rho)g}{k_1\ \mu\ s^2} \frac{\epsilon^3_{mf}}{(1 - \epsilon_{mf})} \qquad (20)$$

The specific particle surface s equals $3/(2d_p)$ for spheres, and the particle number density is proportional to $(1 - \epsilon)$. Also, in most applications, a/δ_0 equals unity. Thus, Equation (20) becomes

$$\Theta \propto \frac{(\Delta\rho)g\ \epsilon^3_{mf}\ (U - U_{mf})}{\mu\ d^2\ (1 - \epsilon_{mf})\ (1 - \epsilon)} \qquad (21)$$

Plotted as a function of superficial velocity, Equation (21) provides for particle-diameter and density dependence in both slope and intercept (or zero point). Therefore, it does not permit the possibility of thermal equilibrium in a two-phase system.

Ruckenstein (*25*) did not develop a specific expression for nominal temperature, but his mean vibration velocity $\overline{v^2}$ should be directly related to thermal energy; for example, $\Theta \propto \overline{mv^2}$.

Thus, the occurrence, explicit or implicit, of a nominal temperature function appears intrinsic to any statistical or kinetic theory analysis of fluidized beds. The restriction that it should be determinable without reference to particle properties has often been overlooked in previous studies.

Parameter Matching

The parameters in the smoothed potential model are readily interpreted for the case of the fluidized bed. The diameter d_p of the fluidized particles can be directly measured, and the free volume v_f can be ascertained through observation of bed-volume expansion.

The free volume per cell in the smoothed potential model, as for hard spheres, is given by Equation (13):

$$v_f = \frac{4\pi}{3}\ \gamma\ (v^{1/3} - v_0^{1/3})^3$$

Thus, the free volume length $(v^{1/3} - v_0^{1/3})$ may be equivalently expressed for fluidized beds in terms of void fraction:

$$v^{1/3} - v_0^{1/3} = v_p^{1/3}\ [(1 - \epsilon)^{-1/3} - (1 - \epsilon_0)^{-1/3}]$$
$$\equiv v_p^{1/3} \cdot f(\epsilon) = v_0^{1/3}\ (1 - \epsilon_0)^{1/3} \cdot f(\epsilon) \qquad (22)$$

This free volume length is directly related to the velocity of the fluid and to the diameter of the fluidized particles. Hence, the kinetic-pressure term in Equation (14) can be evaluated, enabling the viscosity expression of Collins and Raffel to be expressed solely in terms of fluidized-bed parameters. From the measured values of viscosity and from dimensional considerations, a generalized correlation for the temperature parameter can be obtained.

EXPERIMENTAL STUDIES

Apparatus

The general characteristics of the flow system are schematically illustrated by Figure 1. The constant head tank, located 25 ft. above column inlet, served as the water source. Flow control to the column was maintained by three parallel Fischer-Porter rotameters, with the water temperature in all experiments ranging from 20.5° to 23°C. The column itself was made up of an upper and a lower aluminum calming section, each 1 ft. high by 9 in. in diameter, and a center borosilicate glass section 5 ft. high by 9 in. nominal inside diameter.

To improve the horizontal evenness of flow of the entering water, the end of the inlet tube was formed into a sparger and set horizontally, and several evenly spaced holes were drilled on its lower side. Two inches above this was placed a stack of six screen nests, each contained within a brass collar and comprising two 70-mesh screens separated by a ⅜ in. grid stainless steel screen. The entire stack was bolted together and made a watertight fit against the wall of the lower calming section.

The bed support, situated directly between the top of the calming section and the lower edge of the glass section, consisted of two 200-mesh screens separated by two ⅜ in. grid stainless steel screens oriented 45 deg. apart. The lower end of the glass section was tapered; in order to have parallel walls throughout the height of the bed, laminations of polyvinyl acetate were applied as a collar to the inside of the glass.

This relatively large bed is believed adequate to provide a reasonably incisive test of a statistical theory, since it will contain 10^7 fluidized particles or more. The column design is discussed fully by Saxton and Vermeulen (*26*).

Spherical Particles

Glass beads of particle density 2.5 g./cc. were used for all experiments. For each group of runs, the particles were closely sized by screening to within a range of ± 20%, and the arithmetic mean of fifty readings was used to characterize the bed, with the results shown in Table 1.

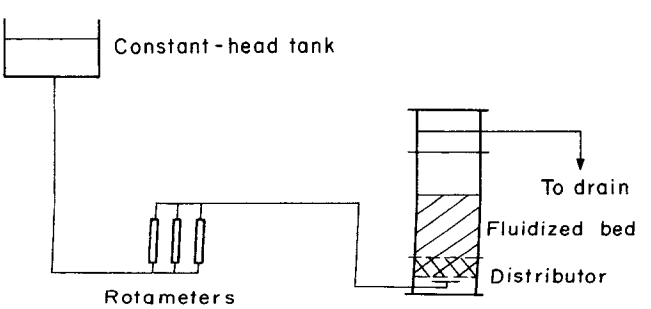

Fig. 1. Flow system.

TABLE 1. GLASS-BEAD SIZES

Bed	d_p, μ	Terminal velocity, cm./sec.	Fixed bed height, in.
A	224	2.94	15.75
B	305	3.94	13.9
C	105	0.85	15.6
D	362	5.5	14.6
E	487	7.4	15.2
F	32	0.082	9.0
G	162	1.67	13.3

Volumetric Behavior

The volumetric behavior of the system may be simply assessed by observing the height of the bed as a function of the fluidizing velocity. To do this, an inch scale was taped to the side of the glass column. It was found that the bed attained equilibrium more rapidly during contraction than during expansion. For this reason, the expansion measurements for the seven particle sizes were made by overexpanding the bed, then measuring the expansion states for a sequence of decreasing fluidizing velocities.

The expansion data obtained are shown in Table 2,* both as void fraction ϵ and as the function $(1 - \epsilon)^{1/3}$ which is related to free volume length by Equation (22).

An indication of the temperature dependence of the free volume length can be gained by plotting $(1 - \epsilon)^{-1/3}$ against the fluidizing velocity U_0, the source of the bed's thermal motion. As shown in Figure 2, $(1 - \epsilon)^{-1/3}$ is linearly dependent upon superficial velocity. All particle sizes have a common intercept at $(1 - \epsilon_0)^{-1/3} = 1.19 \pm 0.010$, or $\epsilon_0 = 0.407 \pm 0.015$.

For comparison, the conventional method of correlating fluidized-bed expansion data by a log-log plot of void fraction against fluidizing velocity is shown in Figure 3. The straightline behavior which is followed conforms to the correlation of Richardson and Zaki, especially at small particle sizes (23).

Viscosity Measurements

Earlier investigations into the apparent viscosity of fluidized beds dealt predominantly with gas systems by using either paddle or cylinder type of viscometers. The former has the inherent disadvantage of causing gross movement within the bed, with the readings becoming dependent on the dimensions of the paddle. Hence, readings would be expected to be greater than those obtained where such gross convection is not present. Although these different methods produce different absolute values, the trends observed are similar; the bed viscosity decreases with increased fluid velocity, decreased particle size, and decreased particle density. Matheson et al. (*19*) also found that spherical particles produced a greater viscosity than irregularly shaped particles in air-fluidized beds. To avoid the gross convection inherent in the gas system, the present experiments have concentrated on liquid systems. The resulting analysis has then been extended to gas systems reported in the literature.

Saxton and Vermeulen (*26*) have shown that the falling ball and rotating spindle viscometers give good qualitative agreement. The present work has employed narrower sized beds to increase the accuracy, using a Brookfield Model LVT "Synchrolectric" viscometer having eight rotational speeds 60, 30, 12, 6, 3, 1.5, 0.6, and 0.3 min.$^{-1}$ for the viscosity measurements, with a single cylindrical spindle. To evaluate the effect of spindle characteristics, preliminary experiments were carried out, with the conclusion that neither bob size nor surface roughness had a significant effect on the viscosity readings. The spindle chosen was a smooth hollow stainless steel cylinder 2.0 in. long with an external diameter of 1.0 and an internal diameter of 0.75 in. This absence of bob-surface effect was postulated to arise from the spheres being coated with a layer of fluid, hence producing effectively soft impacts.

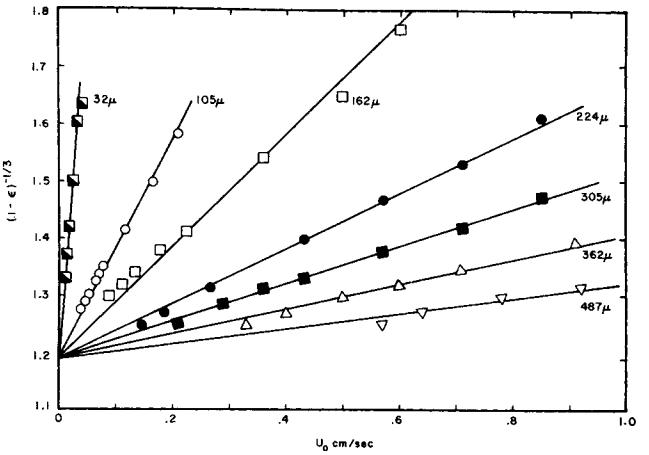

Fig. 2. Dependence of free volume length upon superficial velocity of water and upon particle diameter.

Since the bob geometry was designed so as to minimize the influence of the vertical flow of the fluidizing fluid, resistance to bob rotation should arise almost entirely from these impacts. This premise was confirmed by a series of measurements, made in the absence of particles, which showed that the viscous effect of the flowing fluid alone was at least an order of magnitude less than the smallest values observed in any of the fluidized beds.

The viscometer was mounted on the top plate of the column and could be stationed at two radial locations: center or at 2.0 in. off centerline. The spindle could be situated at various depths in the bed by employing a number of flexible extension wires. For each state of expansion of the bed, values of the deflection α were obtained for the various rotation rates Ω by taking the arithmetic mean of at least thirty consecutive readings. The physical properties of the system were such that only the rotational rates of 30, 12, and 6 rev./min. were meaningful, the values at 60 rev./min. being consistently higher than those predicted by extrapolation of the lower speeds. This was as indicated by the manufacturer's cautions regarding higher speeds and appears due to the initiation of secondary flow (*12*) around the spindle. At speeds lower than 6 rev./min., the percentage error in the readings rendered the values unreliable. In order to obtain some insight into the internal behavior of the bed for each state of expansion, deflection values were obtained at three heights above the distributor, usually 7, 13, and 16 in., and at the two radial locations. In cases

TABLE 2. TYPICAL EXPANSION DATA IN 8.53-IN. COLUMN FOR PARTICLE SIZES INVESTIGATED

Run	U_0, cm./sec.	H, in.	ϵ	$(1 - \epsilon)^{-1/3}$	v, 10^{-6} cc.
A2	0.71	33.6	0.721	1.530	21.8
A5	0.265	21.3	0.560	1.315	13.8
B2	0.71	23.6	0.650	1.418	48.0
B5	0.36	18.75	0.559	1.314	38.0
C2	0.167	31.2	0.702	1.497	2.12
C5	0.072	22.3	0.583	1.338	1.52
D2	0.71	21.1	0.587	1.343	63.6
D5	0.40	17.8	0.511	1.269	53.6
E2	1.06	21.6	0.581	1.336	144
E5	0.64	18.6	0.513	1.271	124
F2	0.034	20.2	0.757	1.602	0.071
F5	0.013	12.5	0.612	1.371	0.044
G2	0.50	33.0	0.776	1.648	10.4
G5	0.18	19.39	0.620	1.380	6.1

* Tables 2 and 4 in complete form, along with Appendix figures and tables, have been deposited as document 00637 with the ASIS National Auxiliary Publications Service, c/o CCM Information Sciences, Inc., 22 W. 34 St., New York 10001 and may be obtained for $1.00 for microfiche or $3.00 for photocopies.

TABLE 3. CALIBRATION OF ANGULAR DEFLECTION READINGS ON BROOKFIELD VISCOMETER

Liquid	Spindle	Spindle rotation = ω rev./min. 30	12	6	3	1.5	0.6	0.3	Brookfield viscosity, centipoise	Spindle slope
Castor oil	Brookfield No. 2	62	24.6	12.2	6.1				614	
	Present work			73.7	36.8	18.6	7.7	3.8		12.28
Mineral oil	Brookfield No. 2	16.5	6.5	3.2					160	
	Present work		40.5	20.2	10.2					3.35
Glycerine	Brookfield No. 3	23.2	11.2	4.5	2.3				500	
	Present work			61.4	31.0	15.7	6.7			10.3
Linseed oil	Brookfield No. 2	10.0	4.9	1.9					49	
	Present work	30.6	12.1	6.0	3.0					1.01

where the expanded height of the bed was greater than 20 in., readings were also taken in at least one other position.

From visual observations, turbulence was noticeable up to a height of 6 to 7 in. above the distributor for all the beds and at various states of expansion. Above this, however, gross convective currents appeared to have subsided. Hence, the readings at 7 in. would be expected to be higher than the others. This was, in fact, found in many cases. At heights just below the bed surface, a thinning effect was found to exist, resulting in lower deflections than those for the central part of the bed. This effect has been shown to exist in both liquid- and gas-fluidized systems [Bakker (*1*), Coeuret (*3*), El Halwagi (*6*)]. The arithmetic average of all readings has been chosen to characterize the bed, that is, to serve as a single representative viscosity value for each state of expansion.

Plots of the shear curves obtained for the beds show nearly Newtonian behavior in practically all cases. To obtain an absolute viscosity value, the spindle was standardized against four Newtonian oils, where viscosity was measured by using the Brookfield charts and standard spindles. Table 3 summarizes these results. A comprehensive tabulation of the shear data for the beds is shown in Table A11.* Values for run F, with $d_p = 32\mu$, were felt to be unreliable and have not been considered further, owing to the shallow bed used and the possible error in the deflections. The absolute viscosities obtained for the other runs are given in Table 4 and Figure 4. The latter, a log-log plot of viscosity against superficial velocity, shows a near linear dependence. This trend was also reported by Furukawa and Ohmae (10) for gas systems.

DISCUSSION

Volumetric Behavior

Equation (18) implies that Θ will increase with U_0 (exponent m being much smaller than 2/3), and hence that $U_0 = 0$ can be taken as the point of zero temperature. Assuming that the temperature function must be independent of individual particle properties, one sees that only zero velocity is energy free, that is, incapable of fluidizing some particle type of very small diameter.

In terms of an abstract model, it is reasonable to expect the void fraction of uniform sphere beds [or other nondimensional properties like the cell volume $(1 - \epsilon)^{-1}$] to converge toward a universal limit as the temperature function Θ goes to zero. As reported above, such a limit is found experimentally for the sphere beds studied, with $\epsilon_0 = 0.407 \pm 0.015$.

A general expression can be established for the dependence of the free volume length upon the independent variables of fluidizing velocity and particle diameter. To determine the particle-diameter dependence, the slopes of the liquid-fluidized-bed expansion curves summarized in Table 5 have been plotted as a function of d_p in Figure 5. (The variation in intercepts seen in Table 5 can be attributed to variations in particle size distribution and shape.) The slope is seen to be inversely proportional to $d_p^{1.59}$. The fit to the expansion data is thus

$$f(\epsilon) = 1.23 \times 10^{-3}\ U_0/d_p^{1.59} \qquad (23)$$

From Equation (22), the free volume length is then

$$v^{1/3} - v_0^{1/3} = 0.99 \times 10^{-3}\ U_0/d_p^{0.59} \qquad (24)$$

How well Equation (23) holds is found by replotting the data of Figure 2 against $U_0/d_p^{1.59}$, as shown in Figure 6. The excellent fit lends support to the premise that the free volume length is a fundamental parameter for fluid-

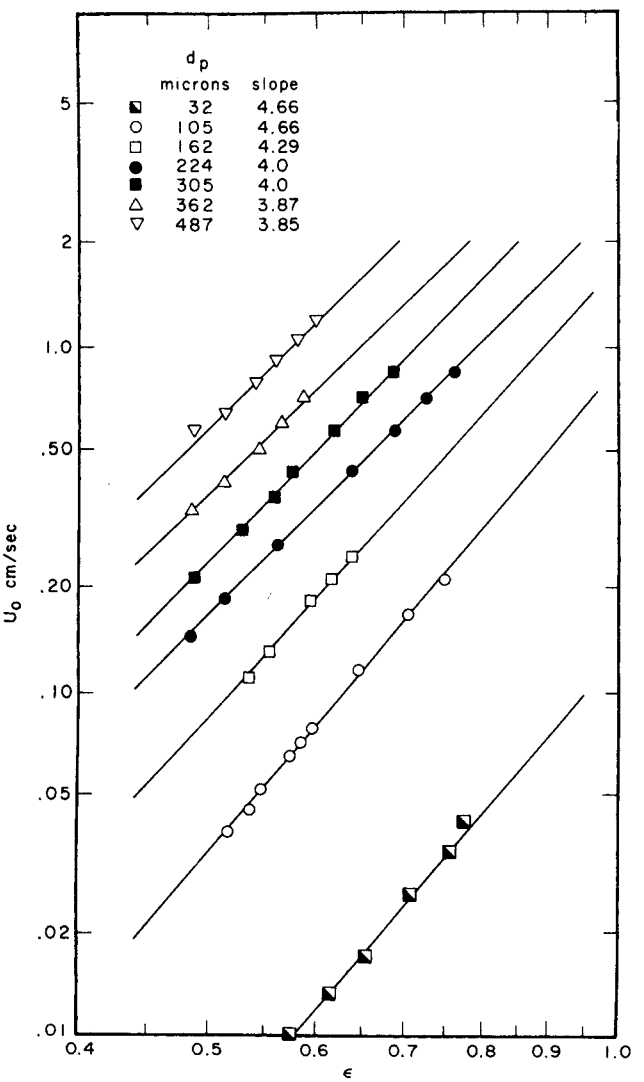

Fig. 3. Dependence of void fraction upon superficial velocity.

* See footnote on p. 123.

TABLE 4. TYPICAL VISCOSITY VALUES (CENTIPOISE) BASED ON MODIFIED BROOKFIELD VISCOMETER

Run	Slope	η
A2	0.40	19.6
A5	0.67	32.8
B2	0.59	28.9
B5	0.792	38.7
C2	0.27	13.2
C5	0.40	19.6
D2	0.82	42.0
D5	1.48	72.5
E2	0.92	45.1
E5	1.70	83.3
G2	0.45	22.1
G5	0.75	36.8

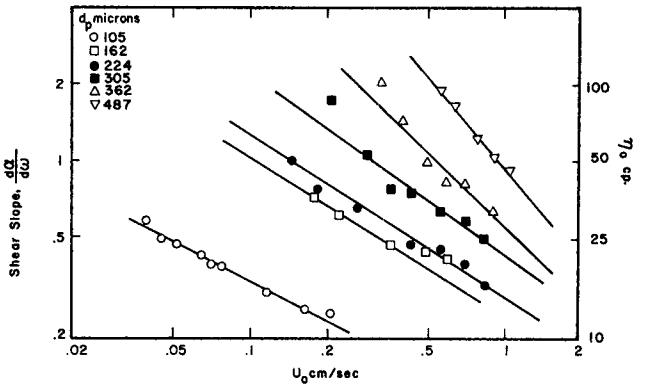

Fig. 4. Shear slope and viscosity as functions of superficial velocity and particle size.

ized beds. That is, the bulk volume behavior matches the type that results if each cell expands in a geometrically fixed manner, as assumed in the cell model.

A more general form of Equation (23) can be established by dimensional analysis and by use of the force balance for a particle in dimensionless form. The resulting relation for voidage function may be written as

$$f(\epsilon) \equiv (1-\epsilon)^{-1/3} - (1-\epsilon_0)^{-1/3} = f(d_p,\ \Delta\rho,\ \rho,\ \mu,\ g,\ U_0) \quad (25)$$

or, in terms of dimensionless groups

$$f(\epsilon) = B_3 \left(\frac{\Delta\rho}{\rho}\right)^{\alpha_1} \left(\frac{\rho U_0 d_p}{\mu}\right)^{\beta_1} \left(\frac{\rho(\Delta\rho)\, g\, d_p^3}{\mu^2}\right)^{\gamma_1} \quad (26)$$

where $\rho U_0 d_p/\mu$ is the Reynolds number N_{Re}, and $\rho(\Delta\rho)g\,d_p^3/\mu^2$ is the Archimedes number N_{Ar}. By comparing Equations (23) and (26), the exponents of the Reynolds number and Archimedes number are easily determined to be $\beta_1 = 1$, $\gamma_1 = -0.86$.

Since measurements were made for only one particle density, determination of the exponent of the density-ratio factor requires additional information. This is available from consideration of the force balance on the particle, which yields for the terminal velocity of a single particle

$$C_D\ u_t^2 = 4\ \Delta\rho\ g\ d_p/(3\rho) \quad (27)$$

In the region of validity of the cell model, the free volume voidage function $[(1-\epsilon)^{-1/3} - (1-\epsilon)^{-1/3}]$ is a measure of the openness of the cell. From the experimental data, this function is proportional to the superficial velocity U_0, the proportionality coefficient being a function of both particles and fluid properties. Therefore, by employing Jahnig's (*14*) argument that the interstitial velocity past a particle in the multiparticle system remains equal to its terminal velocity, the relation between the superficial and terminal velocities is assumed to be

TABLE 5. EXPANSION DATA FROM THE LITERATURE FOR LIQUID-SOLID SYSTEMS

Material	Investigators	Tube diam., cm.	d_p, μ	Slope of $(1-\epsilon)^{-1/3}$ vs. U_0	Intercept $(1-\epsilon_0)^{-1/3}$
Glass beads $\rho_s = 2.49$	Wilhelm and Kwauk (*30*)	7.54	287	0.275	
			510	0.175	1.15
Glass beads $\rho_s = 3.07$	Young (*31*)	3.24	410	0.215	
			482	0.163	1.16
			569	0.135	
Glass beads $\rho_s = 2.45$	Lewis, Gilliland, and Bauer (*18*)	11.4	151	1.07	
			285	0.39	1.18
		6.35	452	0.17	
Glass beads $\rho_s = 2.45$	Hoffman, Lapidus, and Elgin (*13*)	2.54	97	2.05	
			121	1.40	1.21
			191	0.65	
Glass beads $\rho_s = 2.50$	Present work	21.7	32	11.15	
			105	1.694	
			162	0.832	
			224	0.504	1.19 ± 0.01
			305	0.328	
			365	0.245	
			487	0.154	
Sand $\rho_s = 2.68$	Jottrand (*15*)	6.15	43	11.3	
			61	5.85	
			86	2.68	1.25
			113	1.65	
Sand $\rho_s = 2.67$	Wilhelm and Kwauk (*30*)	7.54	373	0.24	
			556	0.156	1.15
			1,000	0.091	

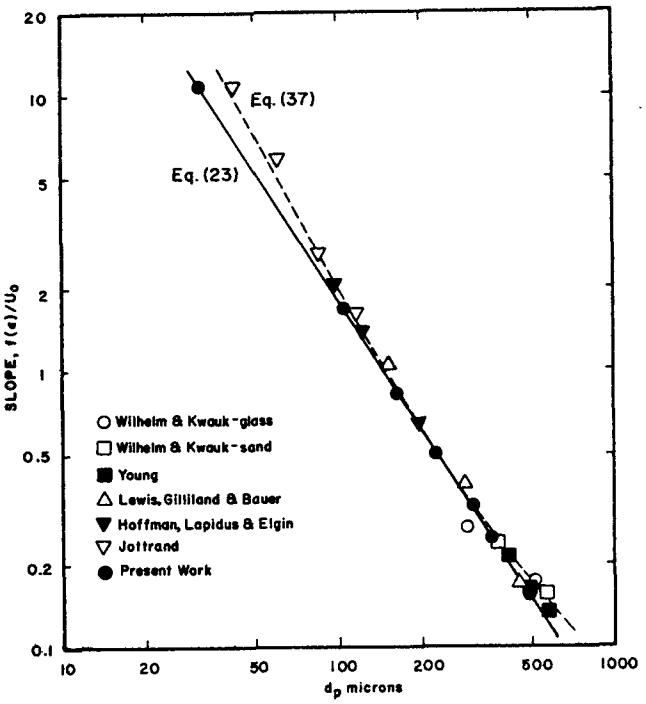

Fig. 5. Particle size effect in bed expansion.

$$U_0 = K u_t f(\epsilon) \tag{28}$$

Also, the drag coefficient C_D may be expressed as

$$C_D = K' \left(\frac{\rho\, u_t\, d_p}{\mu} \right)^{a'} \tag{29}$$

where K' and a' depend on flow regime.

If C_D in Equation (27) is replaced by its equivalent from Equation (29), and u_t is then replaced by its equivalent from Equation (28), the result is

$$\left[\frac{U_0}{K\, f(\epsilon)} \right]^{2+a'} K' \left(\frac{\rho\, d_p}{\mu} \right)^{a'} = \frac{4}{3} \frac{\Delta\rho}{\rho}\, g\, d_p$$

or

$$f(\epsilon) = \frac{U_0}{K} \left[\left(\frac{K'\, 3\rho}{4\Delta\rho\, g\, d_p} \right) \left(\frac{\rho\, d_p}{\mu} \right)^{a'} \right]^{1/(2+a')} \tag{30}$$

Comparison of Equation (30) against Equation (26) with $\beta = 1$ and $\gamma = -0.86$ indicates that the two relations become dimensionally identical if $\alpha_1 = 0$ and $a' = -0.84$. Then, by comparing with Equation (23), $B_3 = 18.8$. Therefore, a general correlation of the expansion data, developed from free volume theory and force balance considerations, is

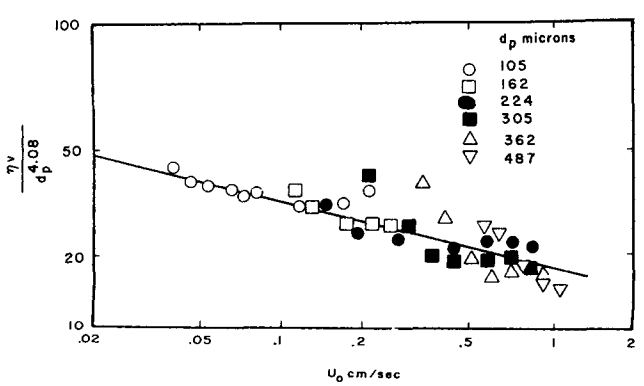

Fig. 7. Viscosity of liquid fluidized bed, compared with Equation (39).

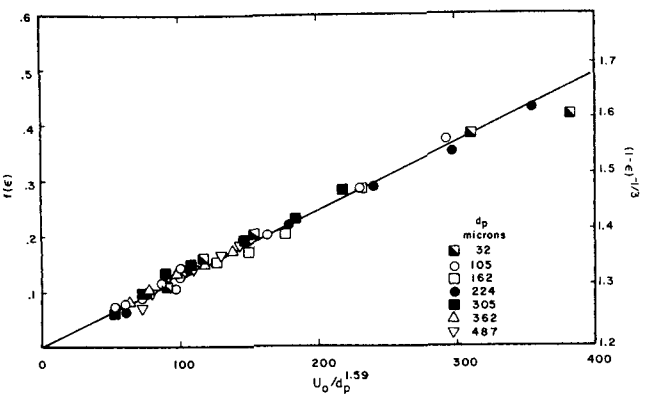

Fig. 6. Voidage correlation function for water fluidized bed of glass beads.

$$f(\epsilon) = 18.8\ N_{Re} \cdot N_{Ar}^{-0.86} \tag{31}$$

This has much the same form as Bena's result for the laminar regime (2), given by

$$\epsilon^{4.65} = 12.8\ N_{Re} \cdot N_{Ar}^{-0.89} \tag{32}$$

This close agreement supports the present density-ratio analysis, since Bena's experimental data encompassed density ratios ($\Delta\rho/\rho$) of 0.2 to 1.5.

Effect of Varying Exponent. A relation more general than Equation (31) is needed to cover the full range of particle densities and fluid properties. The parameters a' and K' are not constant but instead will vary with the terminal-velocity Reynolds number, $\mu\ u_t\ d_p/\mu = N_t$. The known drag-coefficient behavior for single spheres suggests an empirical equation of the following form for a', with the denominator coefficient chosen to give $a' = -0.84$ for 224-μ glass spheres in water:

$$a' = -\frac{1}{1 + 0.080\ N_t^{1/2}} \tag{33}$$

If the voidage function is expressed by a relation having the general form of Equation (23)

$$f(\epsilon) \propto U_0\ d_p^{\zeta} \tag{34}$$

Table 6. Selected Expansion Data for Gas Fluidized Systems

Material	Investigator	Tube diam., cm.	Particle diam., μ	Slope $\times 10^3$ approx.
Glass beads	Lewis, Gilliland,	11.4	102	17.0
$\rho_s = 2.45$	and Bauer (*18*)		155	14.0
			452	4.0
Polyvinyl acetate beads	Furukawa and Ohmae (*10*)	6.0	277	11.8
$\rho_s = 1.3$			324	9.0
			384	7.0
			588	5.9
			755	4.6
Glass beads	Shuster and	15.75	127	21.0
$\rho_s = 2.5$	Haas (*29*)		280	6.4
Glass beads	Schügerl et al.	13.3	70	50
$\rho_s = 2.88$	(*27*)		110	22
			250	10
Plastic beads			250	14.4
$\rho_s = 1.10$				
Sand			275	10.6
$\rho_s = 2.65$			350	8.8

the exponent will vary from -2 to -0.5 as d_p increases, between the Stokes flow and the Newton flow limits, in accordance with the relation [from Equations (26) and (30)]

$$\zeta = 3\gamma_1 + 1 = \frac{a' - 1}{a' + 2} \tag{35}$$

However, since ζ varies with d_p, the slope of Figure 5 between the two limits will not be exactly equal to ζ. Also, N_t is related to N_{Ar} through a' and the undefined K'. It therefore appears preferable to use an empirical bridging function which fits u_t from the Stokes range to the Newton range:

$$f(\epsilon) = A\,(1 + B\,N_{Ar}^{1/2})\,N_{Re}/N_{Ar} \tag{36}$$

where $(1 + B\,N_{Ar}^{1/2})/N_{Ar}$ replaces $N_{Ar}^{\gamma_1}$ in Equation (26). For glass spheres in water, this relation becomes

$$f(\epsilon) = A'\,(1 + B'\,d_p^{3/2})\,U_0/d_p^2 \tag{37}$$

and

$$\frac{d\,\ln\,[f(\epsilon)/U_0]}{d\,\ln\,d_p} = -2 + \frac{1.5\,B'\,d_p^{3/2}}{1 + B'\,d_p^{3/2}} \tag{38}$$

Here $B' = 112$ and $A' = 1.88 \times 10^{-4}$ as evaluated at $d_p = 0.0224$ cm., with a local slope there of -1.59 [as indicated in Equation (23)]. The resulting values for $f(\epsilon)$ are shown by the dashed curve in Figure 5. Similarly, in Equation (36), $B = 0.0294$ and $A = 28.0$ when evaluated at $N_{Ar} = 165$.

Viscosity Behavior

It is important to examine the product of the viscosity and the cell volume as a step toward defining the behavior of the nominal thermodynamic temperature of a fluidized bed. If (ηv) is plotted against U_0, this product shows a mild curvature for small particles and a more extreme curvature for larger ones. Division by a strong function of d_p will group the experimental results so that their plot on logarithmic coordinates, shown in Figure 7, adequately fits a straight line. The empirical equation of this line, weighted toward the smaller particle end, is

$$\frac{\eta v}{d_p^{4.08}} = \frac{18.7}{U_0^{0.25}} \tag{39}$$

The exponent adopted for d_p, 4.08, is determined by the d_p dependence in Equations (26) and (17).

By comparison with Equation (37), the alternate relation can be given:

$$\frac{\eta v}{d_p^{4.50}} = \frac{126}{U^{0.25}\,(1 + 112\,d_p^{1.50})} \tag{40}$$

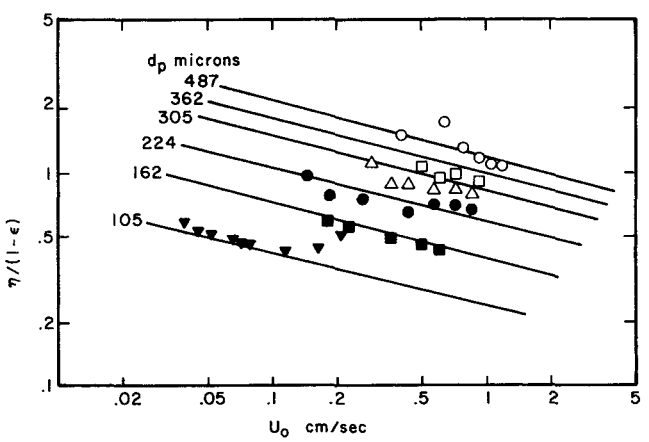

Fig. 8. Viscosity of liquid fluidized bed, compared with Equation (40).

Figure 8 indicates the fit of Equation (40) to the experimental data.

Although Equations (39) and (40) apply only to glass spheres in water at 20°C., they both can be generalized into the following dimensionless form:

$$\left(\frac{\eta v}{\mu\,d_p^3}\right) = \frac{C}{1 + B\,N_{Ar}^{0.50}}\left(\frac{\mu}{d_p\,U_0\,\rho}\right)^{0.25} \left(\frac{\rho(\Delta\rho)\,g\,d_p^3}{\mu^2}\right)^{b'}\left(\frac{\Delta\rho}{\rho}\right)^{0.917} \tag{41}$$

To match Equation (39), $C = 2.72$, $B = 0$, and the Archimedes number exponent b' $(= -0.417 - \gamma_1) = 0.443$. To match Equation (40), $C = 1.90$, $B = 0.0294$, and $b' = 0.583$. The exponent on $(\Delta\rho/\rho)$ is arrived at by the condition, shown in the next section, that the product $(\eta v) \cdot f(\epsilon)$ entering into the statistical temperature function must be proportional to $\Delta\rho^{0.5}$ and $d_p^{2.5}$ but to no other particle parameters.

The total viscosity is essentially the sum of kinetic and collisional contributions. A dilute gas exhibits only kinetic viscosity, given by elementary kinetic theory to be

$$\eta_K = 0.303\,\frac{d_p^{5/2}}{v}\,(\Delta\rho)^{1/2}\,\Theta^{1/2}\,\frac{v^{1/3} - v_0^{1/3}}{v_0^{1/3}} \tag{41a}$$

The collisional viscosity, from Equation (17), is

$$\eta = 0.164\,\frac{d_p^{5/2}}{v}\,(\Delta\rho)^{1/2}\,\Theta^{1/2}\,\frac{v_0^{1/3}}{v^{1/3} - v_0^{1/3}} \tag{41b}$$

Hence, the correction factor for obtaining collisional viscosity from total viscosity should be approximately

$$\frac{\eta}{\eta + \eta_K} \approx \frac{1}{1 + 1.84\,[f(\epsilon)]^2} \tag{41c}$$

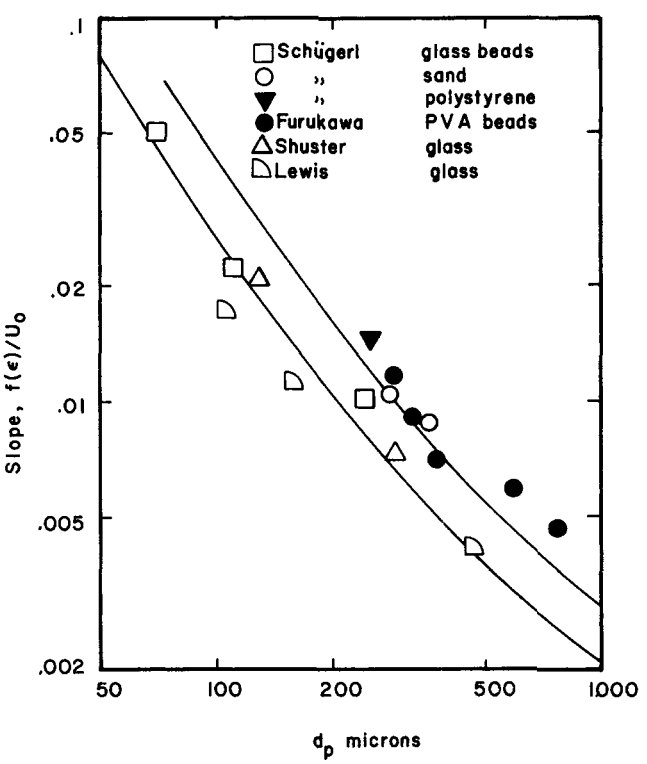

Fig. 9. Expansion of gas fluidized beds, compared with predictions from Equation (36). Upper curve, polyvinyl acetate spheres. Lower curve, glass beads and sand.

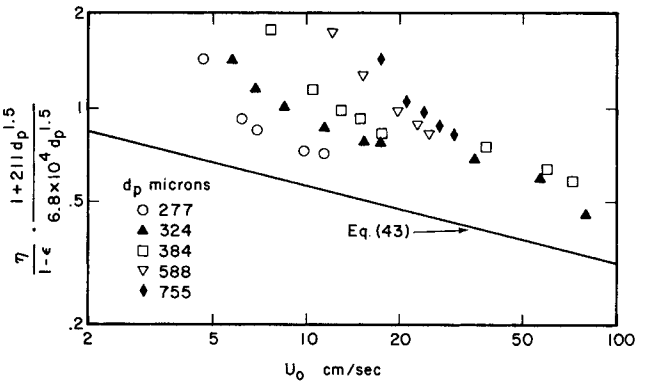

Fig. 10. Viscosity of gas fluidized bed, data of Furukawa and Ohmae, compared with Equation (43).

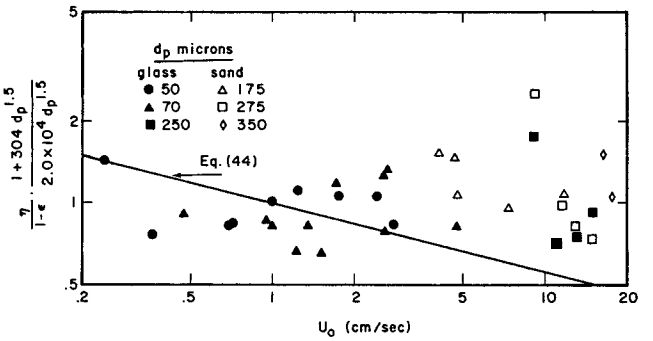

Fig. 11. Viscosity of gas fluidized bed, data of Schügerl, Mertz, and Fetting, compared with Equation (44).

For 224-μ beads and smaller, the departure from 1 should be greatest, and for those runs Equation (41*c*) would predict an increase of about 30% in ηv or $\eta(1-\epsilon)$ from the lowest to the highest U_0 used. The observed increase is no greater than this amount and may be less. Hence, a correction of this type has not been applied to the experimental results.

Comparison of Equation (41) with published experimental systems has been sought. Order-of-magnitude agreement, only, was found between the present theory and the data of Prudhoe and Whitmore (*22*) obtained by falling sphere measurements. In their system the fluidizing medium had a high viscosity (4 poises), and the test spheres had diameters 0.5 to 8 times the diameter of the uniformly suspended particles (0.21 cm.). The measured viscosity, approximately 10 poises, approached the value predicted by the Einstein equation for bulk viscosity of suspensions, whereas 30 to 40 poises would be predicted by Equation (41) with either set of constants. Either the viscosity of the medium or the relatively small size of the measuring element might explain the poor applicability here of the statistical collisional-viscosity approach.

Statistical Temperature

The water fluidized beds of the present study do exhibit expansion and viscosity behavior consistent with a nominal temperature function that is independent of particle diameter. The viscosity equation has been written in a form which assumes also that particle density has no effect on temperature. Combination of Equations (36) (or 31), (22), and (41) into Equation (17) provides a relation matching Equation (18), with $m = 1/6$:

$$\Theta = 6.8 \times 10^4 \frac{\mu^{13/6}\, U_0^{3/2}}{\rho^{7/6}\, g^{5/6}} \qquad (42)$$

The probable physical significance of this temperature function merits a brief comment. The superficial velocity must be used for a particle independent function, but this is closely related to the effective linear velocity and hence to the upper limit for the vibration velocity of the particles. The two fluid velocities appear to have a nearly universal relation:

By definition, $U = U_0/\epsilon$.
From Equation (32), $\epsilon \propto U_0^{1/4.65}$ or $U_0^{0.22}$.
Hence, $U \propto U_0^{1-0.22}$ or $U_0^{0.78}$; also $U_0 \propto U^{1/.78}$ or $U^{1.27}$.
Given $\Theta \propto U_0^{1.5}$, it follows that $\Theta \propto (U^{1.27})^{1.5}$ or $U^{1.91}$.

Within the range of the present data, it is possible that Θ should vary exactly as U^2. In this event, the exponent of U_0 in Equation (42) would be 1.60, and its exponent in Equations (39) to (41) would be 0.20; m in Equation (18) would be 0.133.

According to the definition developed here, a bed for which the cross-sectional area is not constant will have a different nominal temperature at each different cross section.

Extension to Gas Fluidized Systems

The thermodynamic basis for Equation (42) suggests that it should be directly applicable to gas fluidized systems. However, these systems differ somewhat from the particulate model, owing to the separation of gas bubbles at higher velocities which leads to uncertainty in the significance of viscosity results. To minimize this basic difference in the nature of liquid and gas fluidized beds, published data on the latter for bed conditions just above incipient fluidization have been utilized.

Expansion. The gas expansion data from several investigations (see Table 6) exhibit approximately the same intercept of $(1-\epsilon)^{-1/3}$ at $U_0 = 0$, that is, 1.19. The expansion slopes agree well with prediction from Equation (36), as shown in Figure 9. The upper curve shown was computed for $\Delta\rho = 1.3$ and the lower curve for $\Delta\rho = 2.7$. The constants in Equation (37), as derived from Equation (36), are as follows: if $\Delta\rho = 1.3$, then $A' = 3.90 \times 10^{-6}$ and $B' = 211$. If $\Delta\rho = 2.7$, then $A' = 1.88 \times 10^{-6}$ and $B' = 304$. The properties of air used in calculating these values are $\rho = 1.29 \times 10^{-3}$ g./cc. and $\mu = 1.78 \times 10^{-4}$ poise.

Viscosity. To test the liquid-phase theory, the viscosity data of Furukawa and Ohmae (*10*) and of Schügerl et al. (*27*) have been considered in detail. These studies both employed viscometers of a different type from the one used in the present investigation; the effect of such differences, and of possible departures from particle sphericity has not been determined.

Equation (41) has been used to predict the viscosities for air fluidized systems containing polyvinyl acetate or sand. For polyvinyl acetate, the general relation can be put in the form

$$\eta = \frac{6.80 \times 10^3\,(1-\epsilon)\, d_p^{3/2}}{(1 + 211\, d_p^{3/2})\, U_0^{1/4}} \qquad (43)$$

For sand, the explicit expression is

$$\eta = \frac{2.00 \times 10^4\,(1-\epsilon)\, d_p^{3/2}}{(1 + 304\, d_p^{3/2})\, U_0^{1/4}} \qquad (44)$$

In both cases the prediction is consistently low by a factor of almost 2. The results are shown in Figures 10 and 11 and in Tables A12* and A13.* Both viscosity and fluid

* See footnote on p. 123.

velocity in these gas fluidized studies are about fifty times those for the liquid fluidized cases. Thus, the agreement must be considered to be relatively satisfactory and the model to deserve further developmental study.

CONCLUSIONS

A free volume function based on the cell model for simple true liquids is effective in correlating the expansion behavior of liquid fluidized beds and also of gas fluidized systems in the region near minimum fluidization. This function takes into consideration the varying influence of turbulence or of the wakes behind the particles through a complex dependence upon the Archimedes number.

The cell model also gives rise to a collisional-viscosity equation which incorporates the thermodynamic temperature and also incorporates the free volume function. A statistical temperature has been defined in Equation (42) which depends solely upon the physical properties and superficial velocity of the fluidizing medium. Hence, the dependence of the viscosity function upon bed and medium properties is rather narrowly prescribed.

The viscosity function, with its numerical coefficient set at a suitable constant value, fits the viscosities of liquid fluidized systems in their major aspects. It also conforms to the general viscosity behavior of gas fluidized systems but systematically deviates from published values by a factor of about 2.

ACKNOWLEDGMENT

The earlier part of this study, by J. A. Saxton, was carried out in the Lawrence Radiation Laboratory under the auspices of the U.S. Atomic Energy Commission. The later phase, by J. B. Fitton, constituted part of a broad study of rate processes at interfaces, supported by the National Science Foundation.

The authors are grateful to numerous colleagues for helpful discussion and suggestions, including Eugene Petersen, John Beek, R. L. Pigford, Berni Alder, Donald Olander, L. M. Grossman, Robb Hetzler and Michael Williams. Thanks are also due to G. G. Young and Melvin Flamm for equipment design and construction and to Carolyn Saxton and Edith P. Taylor for manuscript preparation.

NOTATION

a = distance between two holes
a = cell radius
a' = exponent in generalized drag coefficient correlation, Equation (29)
A = number of nearest neighbors
A, B, C, A', B' = numerical coefficients
A, B, C, D, E, F = experimental run defined by Table 1
C_D = drag coefficient for free fall
C_4 = constant in Equation (19)
d = Lennard-Jones distance parameter
d_p = particle diameter, cm.
dQ, dS = infinitesimal heat and entropy change
D_T = tube diameter
E = internal energy of system
f = Helmholtz free energy
$f(\epsilon)$ = voidage function, $[(1-\epsilon)^{-1/3} - (1-\epsilon_0)^{-1/3}]$
g = gravitational constant, 981 (cm.)(sec.$^{-2}$)
H = height of bed, in.
H_B = height of spindle, in.
k = Boltzmann's constant
kT = energy equivalent of temperature
K = proportionality constant, Equation (28)
K' = constant in drag coefficient relation, Equation (29)
m = mass of particle
m = empirically determined constant in Equation (18)
n = number of particles (molecules) in subsystem or per volume unit
N = total number of particles in system
N_{Ar} = Archimedes number
N_{Re} = Reynolds number, based on superficial velocity
N_t = Reynolds number, based on terminal velocity
p = pressure
r = radial displacement from cell center
r_0 = centerline position for spindle deflections; r_i = spindle position 2 in. off center
s = specific particle surface
S = entropy
T = absolute temperature
u_t = terminal free fall velocity
U = linear velocity through bed, cm./sec.
U_{mf} = superficial velocity at minimum fluidization
U_0 = superficial velocity, cm./sec.
v = cell volume
v_f = free volume of cell
v_0 = cell volume of closest packing
v_p = particle volume
$\overline{v^2}$ = mean vibrational velocity of Ruckenstein
V = system volume
V_{mf} = bed volume at incipient fluidization
z = molecular partition function
z_{int} = internal partition function
Z = system partition function

Greek Letters

α = Brookfield angular deflection, deg.
α_1 = density ratio exponent
β_1 = Reynolds number exponent
γ = empirical packing factor
γ_1 = Archimedes number exponent
} Equation (27)
δ_0 = distance between centers of adjacent particles
ϵ = void fraction
ϵ_{mf} = void fraction at incipient fluidization
ϵ_0 = void fraction of closest packing
ϵ^* = energy parameter in Lennard-Jones potential
ζ = exponent on d_p in Equation (34)
η = collisional viscosity, poise
η_K = kinetic viscosity, poise
Θ = fluidized bed equivalent of thermodynamic temperature
Λ = thermal factor
μ = fluid viscosity, poise
ρ = fluid density, g./cc.
ρ_s = solid density, g./cc.
$\Delta\rho$ = density difference between solid and fluid
ψ = numerical constant, Equation (18)
Ω = spindle rotation, rev./min.
ω = energy of molecule in average potential field
$\omega(0)$ = configurational energy of particle at cell center
$\omega(r)$ = configurational energy at radial distance r from cell center

LITERATURE CITED

1. Bakker, P. J., and P. M. Heertes, *Chem. Eng. Sci.*, **12**, 260 (1960).
2. Bena, J., *Chemicky Primysl*, 8, No. 10, 516 (1958); *Chem. Abstr.*, **55**, 17117c (1961).
3. Coeuret, F., and P. LeGoff, *Chem. Eng.*, 76 (1967).
4. Collins, F. C., and H. Raffel, *J. Chem. Phys.*, **22**, 1728 (1954); "Advances in Chemical Physics," Vol. 1, p. 135.
5. Diekman, R., and W. Forsythe, *Ind. Eng. Chem.*, **45**, 1174 (1953).
6. El Halwagi, M. M., and A. A. Gomezpata, *AIChE J.*, **13**, 503 (1967).

7. Eyring, H., *J. Chem. Phys.*, **4**, 283 (1936).
8. ———, and J. O. Hirschfelder, *ibid.*, **41**, 249 (1937).
9. Fa-keh, Liu F., and C. Orr, Jr., *J. Chem. Eng. Data*, **5**, 430 (1960).
10. Furukawa, J., and T. Ohmae, *Ind. Eng. Chem.*, **50**, 821 (1958).
11. Haggard, T., and A. M. Sacerdote, *Ind. Eng. Chem. Fundamentals*, **5**, 500 (1966).
12. Hetzler, Robb, and M. C. Williams, *ibid.* (in press).
13. Hoffman, R. F., Leon Lapidus, and J. C. Elgin, *AIChE J.*, **6**, 321 (1960).
14. Jahnig, C. E., paper presented at Am. Inst. Chem. Engrs. meeting, Chicago, Ill. (December, 1957).
15. Jottrand, R., *J. Appl. Chem.*, **2**, Suppl. No. 1, S17 (1952).
16. Kramers, H., *Chem. Eng. Sci.*, **1**, 35 (1951).
17. Lennard-Jones, J. E., and A. F. Devonshire, *Proc. Roy. Soc.*, **A163**, 53 (1937).
18. Lewis, W. K., E. R. Gilliland, and W. C. Bauer, *Ind. Eng. Chem.*, **41**, 1104 (1949).
19. Matheson, G. L., W. A. Herbst, and P. H. Holt, *ibid.*, 1099.
20. Murray, J. D., *Rheologica Acta*, **1**, 6 (1967).
21. Prigogine, I., "The Molecular Theory of Solutions," Interscience, New York (1957).
22. Prudhoe, J., and R. L. Whitmore, *Brit. Chem. Eng.*, **9**, 371 (1964).
23. Richardson, J. F., and W. M. Zaki, *Trans. Inst. Chem. Engrs.*, **32**, 35 (1954).
24. Rosenbluth, M. N., and A. W. Rosenbluth, *J. Chem. Phys.*, **22**, 887 (1954).
25. Ruckenstein, E., *Ind. Eng. Chem. Fundamentals*, **3**, 260 (1964).
26. Saxton, J. A., and T. Vermeulen, *U. S. Atomic Energy Commission Rept. UCRL 11216* (1966).
27. Schügerl, K., M. Mertz, and F. Fetting, *Chem. Eng. Sci.*, **15**, 1 (1961).
28. Scott, G. D., *Nature*, **188**, 908 (1960).
29. Schuster, W. W., and F. C. Haas, *J. Chem. Eng. Data*, **5**, 325 (1960).
30. Wilhelm, R. H., and Mooson Kwauk, *Chem. Engr. Progr.*, **42**, 201 (1948).
31. Young, R. J., *J. Appl. Chem.*, **2**, Suppl. No. 1, S55 (1952).

Manuscript received May 24, 1968; revision received August 20, 1968; paper accepted August 23, 1968. Paper presented at AIChE Los Angeles meeting.

Bubble Coalescence in Fluidized Beds

S. P. LIN

Clarkson College of Technology, Potsdam, New York

The two-dimensional motion of two circular bubbles moving in train up through a fluidized bed is considered. By using continuum equations of motion for this two-phase flow situation, neutral coalescence curves are obtained which indicate, for given bubble radii and distance apart, whether or not the bubbles will coalesce. The conclusions are in agreement with the available experimental results.

In most gas-particle fluidized beds, bubbles or voids of particles pass up through the bed. Empirically it appears that bubbles occur when the ratio of the solid to gas densities is greater than about 10. The gas and particulate motion resulting from the motion of these bubbles is of major importance in particle mixing and in understanding the nature of particle-gas contact. Considerable work has been done on the motion of single bubbles in fluidized beds. Of particular interest from the more fundamental experimental side is the work by Rowe and Partridge and their associates at the Atomic Energy Research Establishment at Harwell. Papers by Rowe and Partridge (*12*) on x-ray studies of bubbles and by Rowe, Partridge, and Lyall (*13*) also give references to previous work and other relevant papers on the experimental side. The latter paper also gives a careful comparison between theory and experiment as of that date. Harrison and Leung (*4*) [see also Davidson and Harrison (*2*)] carried out preliminary experimental work specifically on the coalescence of two-dimensional bubbles moving in train up through a fluidized bed. Their experimental results are compared with the results derived in this paper.

Theoretical studies on the motion (and resulting flows) of single bubbles have been given by Davidson (*1*) [see also Davidson and Harrison (*2*) who give a thorough review of fluidization up to 1962 from both the experimental and theoretical side], Jackson (*5*), and Murray (*7* to *10*). All of these consider continuum flows for both the fluid and particles. Recently, Murray (*10*) considered the unsteady bubble motion investigated experimentally by Partridge and Lyall (*11*); fairly good agreement was found. The flow fields in these situations were shown to be potential flows with constant voidage throughout. The approximate equations he deduced for such situations are linear (because of the Oseenlike approach), simple, and very easy to use. These are given below for the situation under consideration here.

The interesting work by Toei and Matsuno (*14*), which came out after completion of the work in this paper, also treats coalescence theoretically as well as experimentally. Unfortunately, their steady state solutions, obtained on setting $\partial v_s/\partial t = 0$, are not steady since even when the bubbles are in a vertical line, the velocities they find for them are different and thus their distance apart is a function of time, which is an unsteady situation.

EQUATIONS OF MOTION AND SOLUTION

Murray (9, 7) suggested approximate equations of motion for the steady state continuum flow of solids and gas phases in most fluidized beds. These are, in dimensionless form